Sensors and Actuators B 141 (2009) 485–490

Contents lists available at ScienceDirect

Sensors and Actuators B: Chemical

journal homepage: www.elsevier.com/locate/snb

Acoustic wave-based NO_2 sensor: Ink-jet printed active layer

W. Jung*, K. Sahner, A. Leung, H.L. Tuller

Department of Materials Science and Engineering, Massachusetts Institute of Technology, Cambridge, MA 02139, United States

ARTICLE INFO

Article history:
Received 19 March 2009
Received in revised form 27 May 2009
Accepted 3 July 2009
Available online 15 July 2009

Keywords:
Ink-jet printing
QCM
NO_2 sensor
PMMA template

ABSTRACT

Microsphere-templated $BaCO_3$ films with well-defined area were deposited onto quartz crystal microbalances by thermal ink-jet printing, and the devices were characterized with respect to their microstructures and NO_2 sensing characteristics. Highly porous three-dimensional $BaCO_3$ frameworks with promising sensor characteristics were obtained. The printed thin films exhibited reversible frequency shifts following exposure to NO_2 and subsequent recovery under CO/CO_2 at 400 °C. The feasibility of controlled deposition of complex functional films in controlled patterns is discussed in the context of the direct-write features of ink-jet printing.

1. Introduction

Emissions from a variety of sources, including power generation, transportation, and industrial processes are all contributing to the deterioration of indoor and outdoor air quality. This has stimulated interest in the development of improved chemical or gas sensors for both emission monitoring and feedback control. NO_x, in particular, is viewed as a health and environmental hazard given its reactivity with volatile organic compounds to form ozone (smog) leading to respiratory diseases, acid rain and the formation of other toxic chemicals [1]. As a consequence, NO_x air quality standards are being systematically strengthened and are soon likely to reach ppb levels [2], driving the need for even more sensitive sensor devices. Several types of NO_x sensors are under investigation, including chemoresistive sensors based on micro- and nanoscaled semiconductors [3,4] and solid electrolyte based electrochemical sensors [5,6].

A recently proposed alternative approach makes use of the mass change induced in a functional layer when exposed to NO_x [7]. The mass change can be detected using a coated quartz crystal microbalance transducer (QCM) or other acoustic wave devices. Such sensors have recently received increased attention due to their characteristically high sensitivity, relatively low power consumption, and suitability for wireless operation [8,9].

Seh et al. demonstrated the feasibility of using quartz and langasite crystal microbalances as sensing platforms for NO_x at elevated temperatures [7]. At temperatures in the vicinity of 400 °C, earth alkaline carbonates such as $BaCO_3$ transform to nitrates upon NO_2 exposure. The lean-NO_x trap, developed for diesel and lean-burn engines to meet upcoming requirements for significant reduction of NO_x emissions is based on this storage effect [10–12]. The trap is periodically refreshed by running the engine briefly under rich burn conditions, thereby converting the nitrate back to carbonate, and releasing the stored NO_2 as N_2. A NO_x sensor placed at the output of the trap serves to detect the point at which the trap becomes saturated and signals the engine to switch briefly to the rich burn mode.

The amount of $Ba(NO_3)_2$ formed during reaction of NO_2 with $BaCO_3$ is given by:

$$BaCO_3 + 2NO_2 + \tfrac{1}{2}O_2 \rightarrow Ba(NO_3)_2 + CO_2 \quad (1)$$

which increases with the NO_2 partial pressure. The corresponding mass change can be detected using a $BaCO_3$-coated bulk acoustic wave transducer such as a QCM. For small relative mass changes Δm (typically less than several percent), a measurable shift in resonant frequency Δf, proportional to the mass change, is obtained according to the Sauerbrey equation [13]

$$\Delta f = -\frac{f_q^2 \Delta m}{N\rho S} \quad (2)$$

where f_q is the fundamental resonant frequency of the crystal, e.g., quartz, N the frequency constant of the specific crystal cut ($N_{AT} = 1.67 \times 10^5$ Hz cm), ρ the quartz density of 2.65 g/cm^3, and S the surface area covered by the mass-sensitive film.

Improved gas sensitivity is commonly correlated with films exhibiting a large and readily accessible surface area. For this purpose, a microsphere templating technique has been reported for various gas sensitive metal oxides, e.g., In_2O_3 [14], SnO_2 [15], and $CaCu_3Ti_4O_{12}$ [16]. In these studies, the gas sensitive precursors are

* Corresponding author. Tel.: +1 617 721 2703; fax: +1 617 258 5749.
E-mail address: wcjung@mit.edu (W. Jung).

0925-4005/$ – see front matter © 2009 Elsevier B.V. All rights reserved.
doi:10.1016/j.snb.2009.07.010

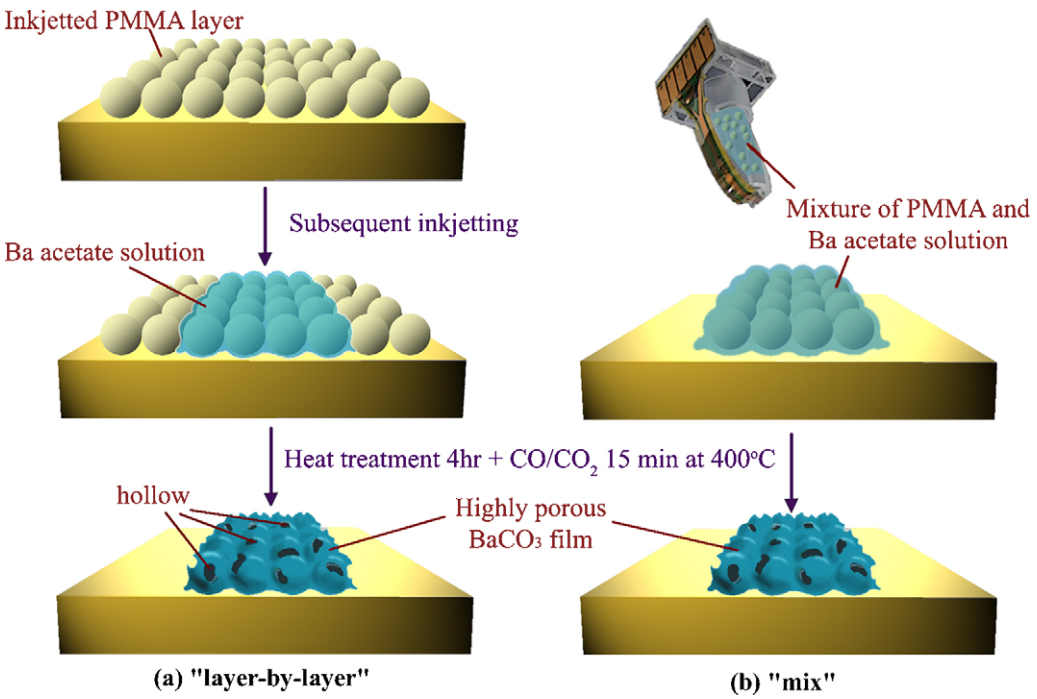

Fig. 1. Schematic diagrams of the two different processing approaches used in this study. (a) The "*layer-by-layer*" approach and (b) the "*mix*" approach.

deposited on top of a 3D array of PMMA microspheres. After subsequent thermal decomposition of the organic template, a porous metal oxide framework is obtained. While this concept was successfully applied by Seh et al. [7] to improve the operation of a QCM based NO_x sensor, a number of important issues relating to reproducibility and optimization remain. In Ref. [7], the procedure for applying the active layer involved dripping a precursor solution by pipette onto the surface of the QCM crystal. As a consequence, one could not achieve accurate confinement of the resultant layer to the center of the QCM, i.e., the mass-sensitive region of the QCM, even with the help of a shadow mask. Furthermore, the pipette limits one to rather large volumes (μl range) of deposited fluid and nonuniform thickness especially near the film edge. Therefore, these factors (off-center, high additional mass, nonuniform film thickness) lead to poor reproducibility, difficulty in optimization, and potential deviations from the linear Sauerbrey equation, thereby deteriorating sensor response [17–19].

To address the need for a convenient, reproducible and low cost method for the deposition of layers onto QCMs, the use of ink-jet printing was investigated. Due to its unique advantages including direct patterning, low cost, potential for high throughput combinatorial chemistry, and low materials waste, this versatile technique has received much attention in recent years [20,21]. This has included the deposition of films for organic LEDs [22], metal electrodes for thin film transistors [23], particle suspensions [24] and complex oxides [25–27].

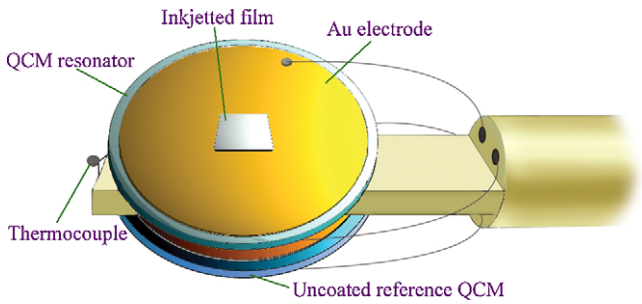

Fig. 2. Schematic illustration of the NO_2 sensing device. The top is the sensor resonator with a coated $BaCO_3$ film while the bottom is the bare reference resonator. A thermocouple is located between the two resonators.

In this study, microsphere-templated $BaCO_3$ films were deposited onto quartz crystal microbalances (QCM) by ink-jet printing and the devices were characterized with respect to their microstructures and NO_2 sensing characteristics. The development of precursor systems for the templated $BaCO_3$ films and the feasibility of utilizing ink-jet printing as a means of achieving well-controlled microstructures suitable for high sensitivity sensor devices are discussed.

2. Experimental

2.1. Sensor preparation

Commercial 6 MHz AT-cut quartz crystal microbalances (Maxtec Inc.), equipped with Au electrodes (0.55 in. in diameter and 150 nm in thickness), served as the resonant platform. The semi-automated thermal ink-jet printer used in this study was provided by Hewlett-Packard for research purposes. For layer deposition, the substrates were positioned on a computer-controlled automated XYZ-stage under the static printhead, thus allowing for the deposition of patterns pixelwise. In the present case, square grid patterns of individual droplets (or "pixels") were printed. The center-to-center spacing between the droplets was adjusted to between 50 and 100 μm. For each pixel, one 55 pl droplet of the respective ink was jetted with a pulse energy of 12.8 μJ from the printer nozzle. Two different approaches, denoted as *layer-by-layer* and *mix*, were tested (see Fig. 1). In either case, each ink was ultrasonicated for several minutes prior to deposition, to ensure homogenization.

The inks for thermal ink-jet printing were prepared using barium acetate (Em Science) and poly methylmethacrylate microspheres (Soken Chemicals, 800 nm diameter) as precursors. For the *layer-by-layer* approach, a layer of PMMA microspheres was first deposited, followed by the gas sensitive $BaCO_3$ precursor. The PMMA loaded ink was prepared by dispersing 1 g of the microspheres in 5 ml of purified water (Millpore Mill-Q, 18.2 MΩ cm). To improve homo-

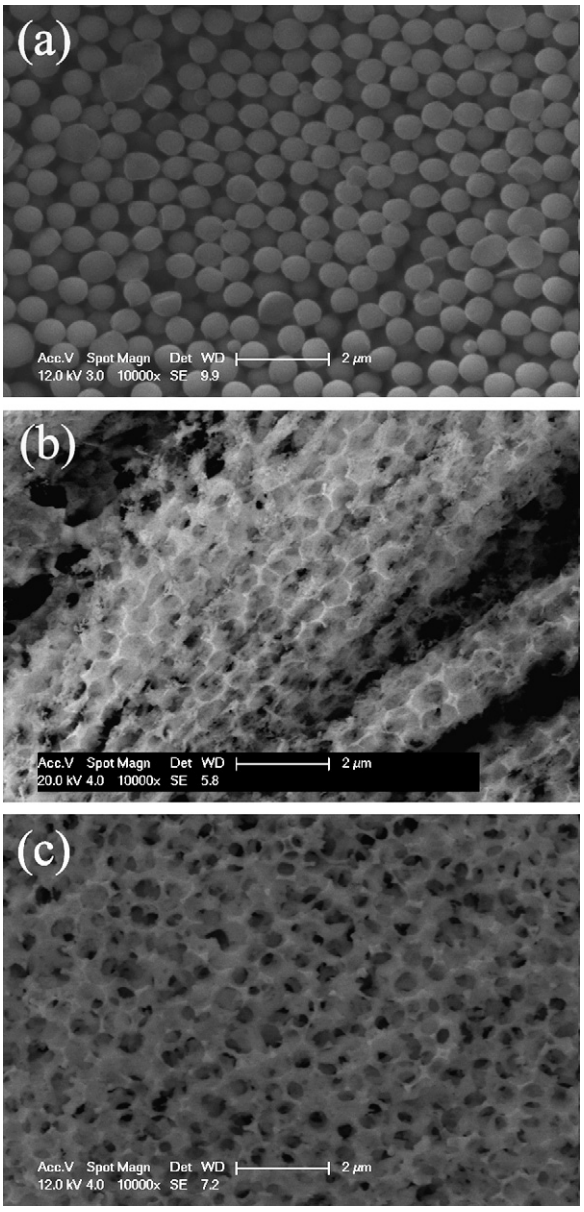

Fig. 3. Scanning electron microscope micrographs of pure PMMA microspheres (a), porous $BaCO_3$ films prepared by *layer-by-layer* approach (b), and by *mix* approach (c).

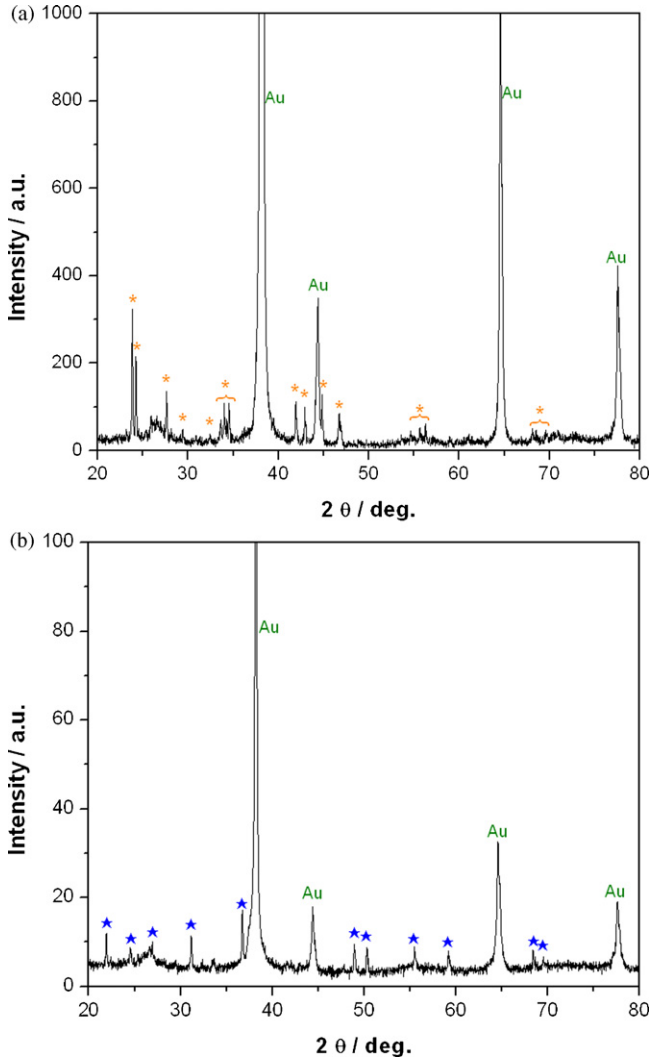

Fig. 4. X-ray diffraction (Cu Kα) patterns of an ink-jet printed $BaCO_3$ film on top of Au electrode prepared by the *mix* approach before (a) and after (b) annealing in 1000 ppm NO_2 in air for 4 h at 400 °C. The symbols (*) and (⋆) represent $BaCO_3$ and $Ba(NO_3)_2$ peaks, respectively.

geneity, stability, and printability of the ink, a thixotropic dispersant (BYK-425, BYK-Chemie, Wesel, Germany) was added (1.2 wt% of the total weight in the mixture) based on the results reported in [28]. The PMMA ink was deposited in a single layer (7 mm × 7 mm). Subsequently, the 3D-PMMA network was covered with three layers (4 mm × 4 mm) of the $BaCO_3$ precursor containing 0.5 g of barium acetate in 4.5 ml of ultra-pure water to form the gas sensitive layer. To this second ink, 0.5 ml of 0.075 M $PtCl_4$ solution was added to activate the sensor layer [7].

For the *mix* technique, a single ink was prepared by mixing the individual components. The barium acetate concentration was adjusted to 0.45 mol/l. The mass ratio between barium acetate and PMMA microspheres was 0.575. Again, the $PtCl_4$ solution and the BYK-425 dispersant were added (0.575 g of Ba acetate + 1 g of PMMA + 0.5 ml $PtCl_4$ solution (0.075 M) + 0.078 g of BYK-425 dispersant + 4.5 ml purified water). The dimensions of the functional layers were 7 mm × 7 mm, 4 mm × 4 mm, and 2 mm × 2 mm with one-layer thickness between 1.5 and 2.5 μm, measured by surface profilometry (Tencor P-16). Both single and double layers were utilized in this study.

For thermal decomposition of the PMMA template, the films were heated at 3 K/min to 400 °C and maintained at that temperature for 4 h. Subsequently they were exposed to a 1:1 CO/CO_2 mixture for 15 min at 400 °C to insure the formation of the barium carbonate phase. Each step is summarized in Fig. 1.

2.2. Sensor testing

$BaCO_3$-coated sensor devices were mounted onto Al_2O_3 sample holders which were inserted inside a quartz tube (G. Finkenbeiner Inc., 22 mm inner diameter, 600 mm length) equipped with inlet and outlet fittings, which in turn was placed into a tube furnace. Pt wires were attached to the Au electrodes on the resonators with the aid of silver paste (SPI Supplies). To minimize cross sensitivity of the resonator frequency to temperature excursions, a bare reference sensor (Maxtec Inc., 6 MHz QCM) was placed adjacent to the coated sensor (see Fig. 2) and its frequency subtracted from that of the coated sensor. This effectively compensated for temperature induced shifts in resonator frequency. The sensors were operated at 400 °C, with the temperature recorded by a thermocouple located

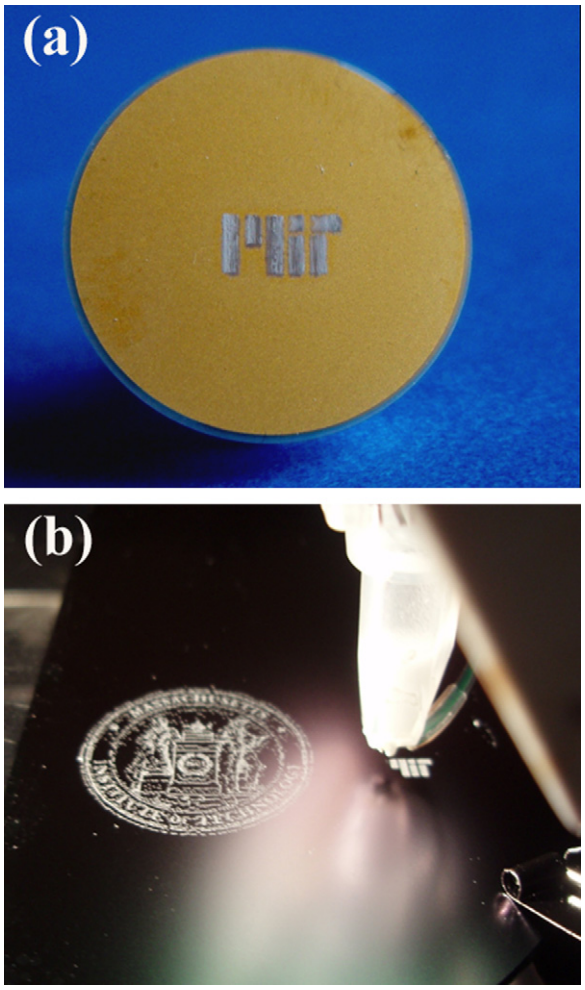

Fig. 5. Examples of the ink-jet printed porous $BaCO_3$ films.

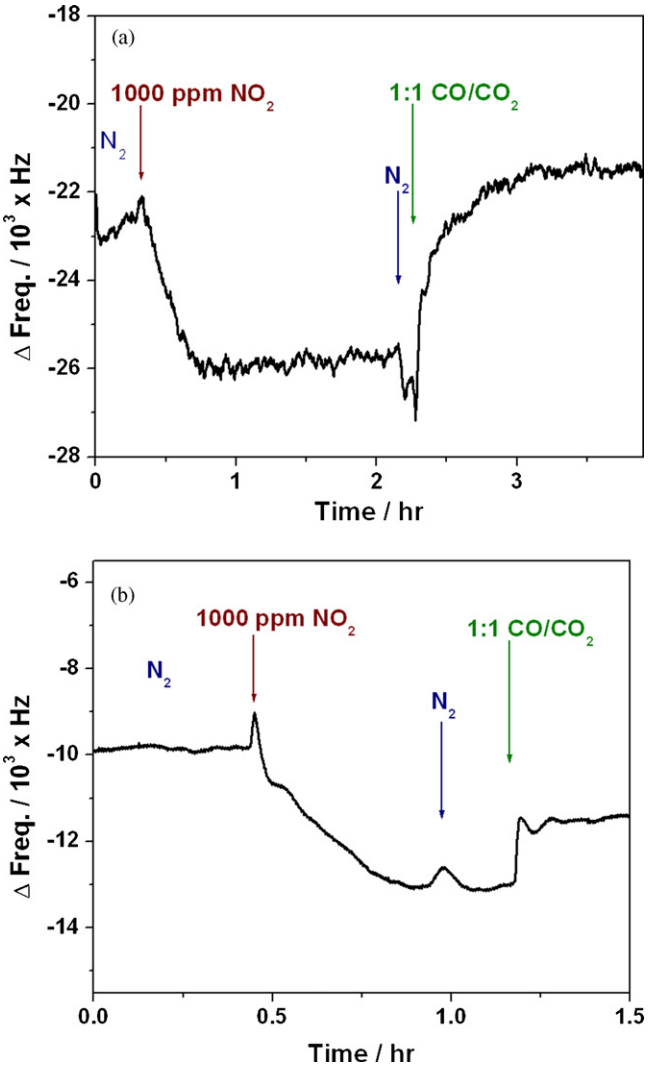

Fig. 6. Sensor response of films to 1000 ppm NO_2 at 400 °C prepared (a) by the *mix* method and (b) by the *layer-by-layer* method.

between the two sensors as shown in Fig. 2. Mass flow controllers (MKS 1359C mass flow controllers and an MKS 647A controller unit) regulated the flow of the different gas mixtures (pure nitrogen for equilibration and flushing, NO_2 (10 ppm and 1000 ppm)/air for response tests, and 1:1 CO/CO_2 mixture for recovery) at a total rate of 100 sccm. The resonant frequency was monitored using the built-in fitting routine (four-element equivalent circuit model) of a network analyzer (Agilent E5100A). Readings were taken approximately every 2 s with the instruments being controlled by Labview (National Instrument) software.

3. Results and discussion

3.1. Film characterization

Fig. 3 presents SEM micrographs of a pure PMMA microsphere layer (a) as well as of the different sensitive films after heat treatment (*layer-by-layer* (b) vs. *mix* (c)). No remaining carbon deposits were observed following the heat treatment, and a highly porous framework was obtained in both cases. By additional XRD characterization, the formation of both the $BaCO_3$ phase after heat treatment and the $Ba(NO_3)_2$ phase after annealing in 1000 ppm NO_2 for 4 h at 400 °C were confirmed as shown in Fig. 4. Pt peaks were not found within the detection limit of the XRD, probably due to the very small levels of added Pt. Even though both films are highly porous, the *mix* film shows better uniformity compared with the film prepared by the *layer-by-layer* approach. Furthermore, the films deposited by

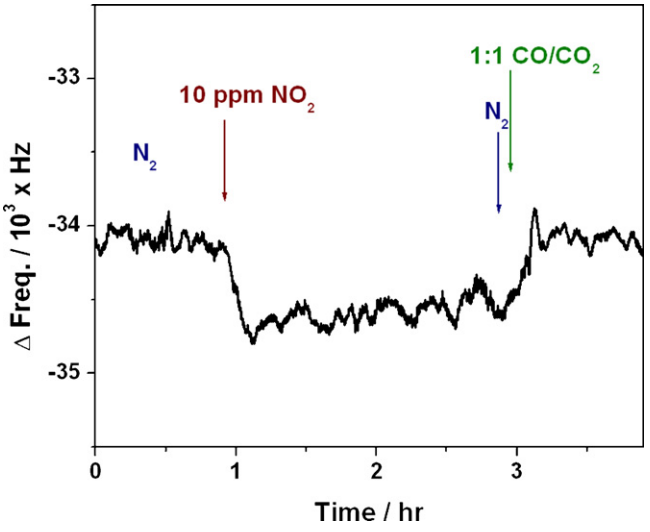

Fig. 7. Sensor response of films to 10 ppm NO_2 at 400 °C prepared by the *mix* method.

the *mix* technique covered the substrate more homogeneously and with improved adhesion.

3.2. Direct patterning and film alignment

For sensors based on QCM or other acoustic wave devices, well-aligned and defined film dimensions are required to prevent potential deviations from the linear Sauerbrey equation (Eq. (2)) and to achieve good reproducibility. In this study, $BaCO_3$ films with uniform thickness and well-defined area were readily obtained by thermal ink-jet printing at the central region of the QCM device. Furthermore, complex $BaCO_3$ film patterns were fabricated, demonstrating the advantage of direct-write processes as shown in Fig. 5. Simple square shaped ink-jet printed $BaCO_3$ films (shown diagrammatically in Fig. 2) were used for the NO_2 sensing studies.

3.3. Sensor tests

The changes in f_o (defined as the difference in frequency between the sensor and the reference, $f_o = f_s - f_{ref}$) of a $BaCO_3$-coated sensor following exposure to NO_2 and subsequent recovery are shown in Fig. 6. Both specimens prepared by either the *layer-by-layer* and the *mix* approach exhibited a clear shift in resonance frequency of ~3.5–4 kHz and reached a stable frequency plateau within approximately 25 min when exposed to 1000 ppm of NO_2. However, the *mix* film showed almost full recovery by subsequent exposure to the CO/CO_2 gas, while the *layer-by-layer* had only ~20% recovery.

Focusing on the *mix* film, the recovery transient initiated by exposure to the CO/CO_2 gas is characterized by a rapid initial increase in frequency followed by a slower transient. This transient response was also observed in the previous study by Seh et al. [7], suggesting a two-step process; rapid kinetics followed by a process characterized by slower kinetics. One may hypothesize that a thin reaction layer of $BaCO_3$ forms quickly, which then serves as a diffusion barrier for subsequent gas diffusion through the reaction product, leading to parabolic diffusion kinetics. However, the transient response by exposure to NO_2 gas showed almost a linear decrease in frequency vs. time. It should be noted that the sensor chamber was relatively large (~200 cm^3) and so the response times may not reflect the true response times of the sensors. This should be considered in light of the fact that the concentration of the oxidant gas NO_2 is much lower than that of reductant gas mixture CO/CO_2 (1000 ppm vs. 50%) and that the recovery kinetics in CO/CO_2 are known to be much slower than the NO_2 response [7,12]. As a consequence, further investigation of the kinetic mechanisms, using a much smaller volume chamber, is currently planned.

The response to a considerably lower level of NO_2 (10 ppm) was also tested with the result shown in Fig. 7. Here, the resonant frequency reached a new lower frequency plateau upon exposure to NO_2 and recovered upon exposure to CO/CO_2 to approximately the initial frequency. Both response and recovery times (10 min and 15 min, respectively) appeared to be somewhat faster than when the sensor was exposed to higher NO_2 concentration (1000 ppm). The shift in resonant frequency is reduced compared to samples exposed to 1000 ppm NO_2 (~580 vs. ~4000 Hz), as would be expected given the reduced mass of carbonate converted to nitrate. However, a simple linear relation between the frequency change and NO_2 concentration was not found. As discussed later, this behavior is attributed to a saturation of the $BaCO_3$ film upon exposure to 1000 ppm NO_2. Signal noise is related to local temperature fluctuations not entirely compensated by the use of the compensating uncoated resonator as confirmed by in situ temperature measurements.

3.4. Complete and partial conversion from $BaCO_3$ to $Ba(NO_3)_2$ by NO_2

Ink-jet printing provides precise control of the total deposited amount of the active layer. This is achieved by careful control of the deposition parameters such as nozzle size, pulse energy, and pulse frequency. From the well-defined volume of each droplet (55 pl), the total number of deposited droplets, and the concentration of each element in the precusor solution (i.e., 200 g/l of PMMA and 0.45 mol/l of Ba acetate), the exact amount of each deposited element can be precisely determined. Therefore, based on the ink-jet deposition parameters, it was possible to calculate Δx_{dep} corresponding to the molar amount of $BaCO_3$ deposited onto the quartz crystal.

By measuring changes in f_o, the corresponding mass changes per m^2 (Δm_{area}) of the active films can also be calculated using the Sauerbrey equation (Eq. (2)). Because ink-jet printing precisely defines the covered area S, the absolute mass change $\Delta m = S\Delta m_{area}$ can be accurately calculated. Therefore, the molar amount of barium carbonate converted to barium nitrate, Δx_{conv}, is given by

$$\Delta x_{conv} = \frac{\Delta m}{\Delta\,[M(\mathrm{Ba(NO_3)_2}) - M(\mathrm{BaCO_3})]} \tag{3}$$

with the molar weights of the barium compounds given by $M(Ba(NO_3)_2) = 261.3$ g/mol and $M(BaCO_3) = 197.34$ g/mol.

Δx_{dep} and Δx_{conv} values from four different samples used in this work are summarized in Table 1 along with the sample dimension and the corresponding changes in f_o. These data enable one to determine the percentage of $BaCO_3$ converted to $Ba(NO_3)_2$ upon exposure to NO_2. In all of the samples exposed to 1000 ppm NO_2, all of the $BaCO_3$, within experimental error, is converted to $Ba(NO_3)_2$ (see Table 1). This implies that carbonate films exposed to 1000 ppm NO_2 gas fully react to form the nitrate, thereby establishing an upper limit of NO_2 concentration that can be detected by such a sensor device. It needs be noted that regardless of process and film geomtry (area, number of layers, and droplet spacing), all films show nearly complete conversion to $Ba(NO_3)_2$ when exposed to 1000 ppm NO_2 for periods of time greater than about 25 min.

On the other hand, exposure to 10 ppm NO_2 results in a very different response. Here, only ~5% of the $BaCO_3$ was converted into $Ba(NO_3)_2$, corresponding to a frequency change of 580 Hz. This result suggests that at these concentrations, the device can work in a sensor rather than just a detector mode.

Table 1
Summary of deposition parameters and NO_2 responses for four samples used in this work. Deposited Δx_{dep} and calculated Δx_{conv} represent the total molar amount of deposited $BaCO_3$ and the molar amount of $BaCO_3$ converted into $Ba(NO_3)_2$ estimated from the total deposited volume and the frequency shift, respectively.

Approach	Area [cm^2]	Number of layers	Droplet spacing [μm]	Δf_o [Hz]	Calculated Δx_{conv} [mol]	Deposited Δx_{dep} [mol]	Conversion ratio [%]
Layer-by-layer	0.16	3	100	3500	1.08×10^{-7}	1.05×10^{-7}	103
Mix	0.49	1	60	4000	3.76×10^{-7}	3.56×10^{-7}	106
Mix	0.16	1	50	4600	1.41×10^{-7}	1.59×10^{-7}	89
Mix	0.04	2	50	580	4.46×10^{-9}	8.31×10^{-8}	5

4. Conclusion

Microsphere-templated $BaCO_3$ films were deposited onto a QCM device by thermal ink-jet printing and their sensor responses were investigated by monitoring changes in resonant frequency. Two different approaches, *layer-by-layer* and *mix*, were utilized for the film depositions. Both techniques successfully provided highly porous three-dimensional $BaCO_3$ frameworks, but the *mix* technique showed superior film uniformity and adhesion to the QCM crystal. The ink-jet printing approach offered a means of highly controlled spatial deposition of the film as well as the total molar amount of the precursor film materials.

The printed thin films exhibited reversible frequency shifts following exposure to NO_2 and subsequent recovery by CO/CO_2 at 400 °C, as expected based on the operation of the lean-NO_x trap. A careful examination of the molar fraction of barium carbonate converted to barium nitrate, Δx_{conv}, as determined from the frequency shift, showed that at high NO_2 levels (1000 ppm), all of the carbonate was converted to nitrate in a relative short period of time leading to saturation of the sensor. On the other hand, exposure to reduced NO_2 levels (10 ppm) results in only a small fraction of the $BaCO_3$ being converted into $Ba(NO_3)_2$, offering the possibility for the device to work in a sensor rather than just a detector mode.

Further investigations, using small volume reaction chambers and controlled NO_2 concentrations, e.g., 1–100 ppm, should allow for a more careful in situ examination of the kinetics of both nitrate formation upon exposure of the carbonate to NO_2 and carbonate formation upon exposure of the nitrate to lean-burn conditions.

Acknowledgements

This work was supported by the MIT-OSU-HP Focus Center on Non-Lithographic Technologies for MEMS/NEMS under grant HR0011-06-1-0045. WooChul Jung gratefully acknowledges financial support of the Samsung Scholarship. Kathy Sahner gratefully acknowledges financial support of the Bavarian Science Foundation, Germany (grant PDOK 29/05). The authors thank Prof. Vladimir Bulovic and Dr. Jianglong Chen, MIT for use of a computer-controlled automated XYZ-stage, Hewlett-Packard for use of an ink-jet head, and Dr. Luanne Rolly and Dr. Tom Etheridge for constructive discussions.

References

[1] http://www.epa.gov/air/urbanair/nox/hlth.html.
[2] D. Zhang, Z. Liu, C. Li, T. Tang, X. Liu, S. Han, B. Lei, C. Zhou, Detection of NO_2 down to ppb levels using individual and multiple In_2O_3 nanowire devices, Nano Lett. 4 (2004) 1919–1924.
[3] I.D. Kim, A. Rothschild, B.H. Lee, D.Y. Kim, S.M. Jo, H.L. Tuller, Ultrasensitive Chemiresistors Based on Electrospun TiO_2 Nanofibers, Nano Lett. 6 (2006) 2009–2013.
[4] A. Maiti, J.A. Rodriguez, M. Law, P. Kung, J.R. McKinney, P. Yang, SnO_2 nanoribbons as NO_2 sensors: insights from first principles calculations, Nano Lett. 3 (2003) 1025–1028.
[5] G.M. Kale, L. Wang, J.E. Hayes, J. Congjin, Y.R. Hong, Solid-state sensors for in-line monitoring of NO_2 in automobile exhaust emission, J. Mater. Sci. 38 (2003) 4293–4300.
[6] J. Yoo, E.D. Wachsman, NO_2/NO response of Cr_2O_3 and SnO_2 based potentiometric sensors and temperature-programmed reaction evaluation of the sensor elements, Sens. Actuators, B, Chem. 123 (2007) 915–921.
[7] H. Seh, T. Hyodo, H.L. Tuller, Bulk acoustic wave resonator as a sensing platform for NO_x at high temperatures, Sens. Actuators, B, Chem. 108 (2005) 547–552.
[8] W.E. Bulst, G. Fischerauer, L. Reindl, State of the art in wireless sensing with surface acoustic waves, IEEE Trans. Ind. Electron. 48 (2001) 265–271.
[9] J.D.N. Cheeke, Z. Wang, Acoustic wave gas sensors, Sens. Actuators, B, Chem. 59 (1999) 146–153.
[10] P. Forzatti, I. Nova, L. Castoldi, NO_x removal catalysis, Chem. Biochem. Eng. Q 19 (2005) 309–323.
[11] C.M.L. Scholz, V.R. Gangwal, J. Hoebink, J.C. Schouten, NO_x storage/reduction over lean-burn automotive catalysts, Appl. Catal. B: Environ. 70 (2007) 226–232.
[12] U. Tuttlies, V. Schmeisser, G. Eigenberger, A new simulation model for NO_x storage catalyst dynamics, Top. Catal. 30–31 (2004) 187–192.
[13] V.M. Mecea, Is quartz crystal microbalance really a mass sensor? Sens. Actuators, A, Phys. 128 (2006) 270–277.
[14] B. Li, Y. Xie, M. Jing, G. Rong, Y. Tang, G. Zhang, In_2O_3 hollow microspheres: synthesis from designed $In(OH)_3$ precursors and applications in gas sensors and photocatalysis, Langmuir 22 (2006) 9380–9385.
[15] T. Hyodo, K. Sasahara, Y. Shimizu, M. Egashira, Preparation of macroporous SnO_2 films using PMMA microspheres and their sensing properties to NO_x and H_2, Sens. Actuators, B, Chem. 106 (2005) 580–590.
[16] I.D. Kim, A. Rothschild, T. Hyodo, H.L. Tuller, Microsphere templating as means of enhancing surface activity and gas sensitivity of $CaCu_3Ti_4O_{12}$ thin films, Nano Lett. 6 (2006) 193–198.
[17] C. Hess, K. Borgwarth, J. Heinze, Integration of an electrochemical quartz crystal microbalance into a scanning electrochemical microscope for mechanistic studies of surface patterning reactions, Electrochim. Acta 45 (2000) 3725–3736.
[18] A.C. Hillier, M.D. Ward, Scanning electrochemical mass sensitivity mapping of the quartz crystal microbalance in liquid media, Anal. Chem. (1992) 2539–2554.
[19] X. Tu, Q. Xie, C. Xiang, Y. Zhang, S. Yao, Scanning electrochemical microscopy in combination with piezoelectric quartz crystal impedance analysis for studying the growth and electrochemistry as well as microetching of poly(o-phenylenediamine) thin films, J. Phys. Chem. B (2005) 4053–4063.
[20] J.R.G. Evans, Direct ink jet printing of ceramics: experiment in teleology, Br. Ceram. Trans. 100 (2001) 124–128.
[21] J.R.G. Evans, M.J. Edirisinghe, P.V. Coveney, J. Eames, Combinatorial searches of inorganic materials using the ink-jet printer: science, philosophy and technology, J. Eur. Ceram. Soc. 21 (2001) 2291–2299.
[22] M. Bale, J.C. Carter, C.J. Creighton, H.J. Gregory, P.H. Lyon, P. Ng, L. Webb, A. Wehrum, Ink-jet printing: the route to production of full-color P-OLED displays, J. Soc. Inf. Display 14 (2006) 453–459.
[23] D. Kim, S. Jeong, S. Lee, B.K. Park, J. Moon, Organic thin film transistor using silver electrodes by the ink-jet printing technology, Thin Solid Films 515 (2007) 7692–7696.
[24] J.R.G.E. Mohammad Masoud Mohebi, Combinatorial ink-jet printer for ceramics: calibration, J. Am. Ceram. Soc. 86 (2003) 1654–1661.
[25] S. Okamura, R. Takeuchi, T. Shiosaki, Fabrication of ferroelectric $Pb(ZrTi)O_3$ thin films with various Zr/Ti ratios by ink-jet printing, Jpn. J. Appl. Phys. 41 (2002) 6714–6717.
[26] J.C.H. Rossiny, S. Fearn, J.A. Kilner, Y. Zhang, L. Chen, Combinatorial searching for novel mixed conductors, Solid State Ionics 177 (2006) 1789–1794.
[27] J. Wang, M.M. Mohebi, J.R.G. Evans, Two methods to generate multiple compositions in combinatorial ink-jet printing of ceramics, Macromol. Rapid Commun. 26 (2005) 304–309.
[28] Y. Zhang, L. Chen, S. Yang, J.R.G. Evans, Control of particle segregation during drying of ceramic suspension droplets, J. Eur. Ceram. Soc. 27 (2007) 2229–2235.

Biographies

WooChul Jung received his BE in material science and engineering in 2004 from Seoul National University, Korea and is currently pursuing PhD degree in material science and engineering at MIT, USA. His research interest includes the processing and characterization of thin film based solid state ionic devices (sensors and solid oxide fuel cell).

Kathy Sahner received her German engineering diploma in materials science from the Saarland University, Germany, in 2002. At the same time, she also received the corresponding French degree from the European School of Materials Science and Engineering (EEIGM), France. During her PhD, she investigated gas sensitive perovskites including mechanistic modeling. She then worked as a postdoctoral researcher at the University of Bayreuth, Germany, and at the Massachusetts Institute of Technology, USA, on various projects within the field of electroceramics and ion conductors. She now works at Robert Bosch R&D.

Amy Leung is currently studying chemical engineering at MIT, USA. She plans to graduate in 2010 with a Bachelor of Science Degree. She has been involved in research on polyelectrolyte multilayer drug delivery coatings for intraocular lens.

Harry L. Tuller received his SB and SM degrees in electrical engineering and his engineering science doctorate in solid state science and engineering from Columbia University in New York. He served as postdoctoral fellow in physics at the Technion, Haifa, Israel. He is a member of the faculty of the Department of Materials Science and Engineering at MIT, where he serves as professor of ceramics and electronic materials and director of the Crystal Physics and Electroceramics Laboratory. Dr. Tuller's current research emphasizes the modelling, processing, characterization and optimization of solid state ionic devices (sensors, batteries, fuel cells). He has published over 330 articles and co-edited 12 books. Dr. Tuller has been awarded 21 patents. Dr. Tuller is editor-in-chief of the Journal of Electroceramics and series editor of Electronic Materials: Science and Technology, Springer Publishers. He is a Fellow of the American Ceramic Society, recipient of Fulbright and von Humboldt Awards and former holder of the Sumitomo Electric Industries Faculty Chair at MIT. He served as visiting professor at the Universite Pierre et Marie Curie in Paris and visiting fellow at Imperial College, London and the Max Planck Institute in Stuttgart, Germany. Dr. Tuller was awarded *docteur honoris causa* in 2004 by the University of Provence, Marseilles, France and in 2009 by the University of Oulu, Finland. Dr. Tuller is co-founder of Boston MicroSystems Inc., a pioneer in the design and fabrication of harsh environment compatible micromachined Si and SiC-based sensor arrays.